Lipopeptide antibiotics disrupt interactions of undecaprenyl phosphate with UptA

Abraham O. Oluwole[1,2*], Neha Kalmankar[1,2], Michela Guida[2,3], Jack L. Bennett[1,2], Giovanna Poce[3], Jani R. Bolla[2,4] Carol V. Robinson[1,2*]

[1]Department of Chemistry, University of Oxford, South Parks Road, Oxford, OX1 3QZ, UK. [2]The Kavli Institute for Nanoscience Discovery, Oxford, South Parks Road, Oxford, OX1 3QU, UK. [3]Department of Chemistry and Technologies of Drug, Sapienza University of Rome, 00185 Rome, Italy. [4]Department of Biology, University of Oxford, South Parks Road, Oxford, OX1 3RB, UK.

Email: abraham.oluwole@chem.ox.ac.uk; carol.robinson@chem.ox.ac.uk

Abstract: The peptidoglycan pathway represents one of the most successful drug targets with the last but critical step being the recycling of undecaprenyl phosphate. This translocation of undecaprenyl phosphate is facilitated by DedA and DUF386 domain-containing family membrane proteins via unknown mechanisms. Here we employ native mass spectrometry to investigate the interactions of *Bacillus subtilis* UptA, a putative C_{55}-P flippase, with C_{55}-P, membrane phospholipids and cell wall targeting antibiotics. Our results show that UptA, expressed and purified in *E. coli*, forms monomer-dimer equilibria, and binds to ligands in a pH-dependent fashion. Specifically, we show that UptA interacts more favourably with C_{55}-P over shorter-chain analogues and membrane phospholipids. Moreover, we demonstrate that lipopeptide antibiotics, amphomycin and aspartocin D, can directly intercept UptA function by outcompeting the substrate for the protein binding site. Overall, this study suggests that UptA-mediated translocation of C_{55}-P is potentially regulated by anionic phospholipids and provides insights for future development of antibiotics targeting carrier lipid recycling.

Introduction

The global threat of drug-resistant bacterial pathogens calls for renewed efforts in the search for new antibiotics, along with the identification of new biochemical pathways and interactions that can be effectively targeted. A key antibiotic target is peptidoglycan, the cell wall polymer that provides bacteria with resistance to osmotic stress and environmental assaults (1, 2). Accordingly, topline antibiotics such as amoxicillin and vancomycin (3, 4) intercept the transpeptidation step of the peptidoglycan synthesis (5-7). Moreover, promising antibiotic candidates, such as ramoplanin and moenomycin, target the transglycosylation step (8, 9). Peptidoglycan biosynthesis begins with the formation of UDP-*N*-acetylmuramyl-pentapeptide in the cytosol (10), followed by its coupling to the lipid carrier undecaprenyl monophosphate (C_{55}-P) on the cytosolic side of the inner membrane (Fig.1A) (11, 12). The resulting lipid I is further decorated with a GlcNAc residue to form lipid II (13) before being flopped across the inner membrane (14-16). In the periplasm, the glycopeptide moieties of lipid II are cross-linked into a nascent peptidoglycan polymer and the lipid carrier is released as undecaprenyl diphosphate (C_{55}-PP) (17-19). To participate in the next round of precursor transfer, C_{55}-PP must be dephosphorylated to form C_{55}-P (20-22) and then flipped across the inner membrane such that its phosphate headgroup returns to the cytoplasmic side. The mechanism by which C_{55}-P is translocated across the cytoplasmic membrane is the least understood of the membrane-associated steps of the peptidoglycan pathway (Fig. 1A).

Recently, proteins belonging to the DedA- and the DUF368 domain-containing families were shown to facilitate trans-bilayer transport of C_{55}-P in the Gram-positive bacteria *Bacillus subtilis* and *Staphylococcus aureus* (23), and in the Gram-negative bacteria *Vibrio cholerae* (24). DedA proteins are highly conserved, having 8 homologues in the model bacteria *E. coli* and 6 homologues in *B. subtilis*, respectively (25-27). *B. subtilis* DedA paralogues include UptA and PetA, which are proposed to facilitate trans-bilayer flipping of C_{55}-P and anionic phospholipids, respectively (23, 28). The DUF368-domain containing proteins, exemplified by PopT, are less conserved, being found in *S. aureus* and *V. cholerae*, but are absent in *B. subtilis* and *E. coli* (29). *V. cholerae* PopT becomes essential for cell survival only in alkaline conditions (24). Several Gram-positive and Gram-negative bacteria encode one or multiple UptA-type transporters suggesting that C_{55}-P recycling, mediated by these flippases, is broadly conserved across different bacterial species. For example, the single DedA homologue in *Borrelia burgdorferi* is an essential protein required for proper cell division in this organism (30). Accordingly, the recycling step of peptidoglycan biosynthesis mediated by UptA-type flippases can be targeted by antibiotics. This necessitates a molecular-level understanding of how UptA interacts with its cognate substrate, C_{55}-P, and potentially with membrane phospholipids, to elucidate the mechanism of C_{55}-P translocation for antibiotic targeting.

Herein we employ native mass spectrometry to elucidate how *B. subtilis* UptA interacts with multiple lipidic substrates and antibiotics. We show that purified UptA exists as an equilibrium of monomers and dimers. We further show that UptA interacts more favourably with C_{55}-P than C_{55}-PP and membrane phospholipids and

provide molecular-level evidence on the amino acid residues involved in C_{55}-P binding. We find that UptA binds to its cognate ligand C_{55}-P in a pH-dependent manner and show that lipopeptide antibiotics, such as amphomycin and aspartocin D, bind to UptA with higher affinity than other cell-wall targeting antimicrobial peptides. Interestingly, these lipopeptides can intercept peptidoglycan biosynthesis by out-competing the flippase for C_{55}-P, highlighting avenues for the development of novel antibiotics.

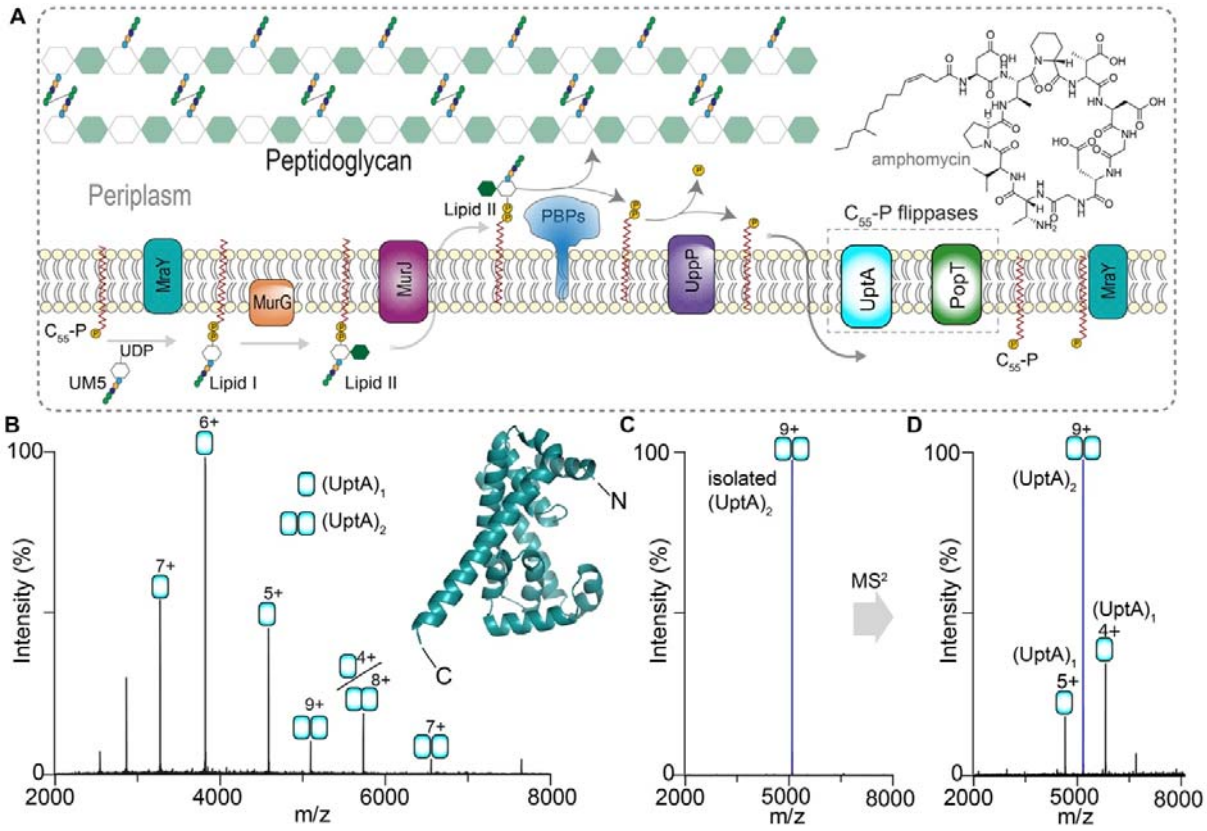

Fig. 1: UptA is primarily monomeric with a low population of dimer. A) A schematic depiction of the lipid II cycle of peptidoglycan biosynthesis. **B**) Native mass spectrum of UptA (2.2 µM) liberated from a buffer containing 200 mM ammonium acetate (pH 8.0), 0.05% LDAO. Peaks are assigned to UptA in monomeric and dimeric forms. Insert, the model structure of UptA (AFO31823-F1) predicted by AlphaFold (31). Predicted N- and C- termini are indicated. **C**) Quadrupole isolation of the UptA dimer (9+ charge state). **D**) MS/MS of the isolated UptA dimer charge state upon collisional activation (190 V). The dimer dissociates into individual UptA protomers confirming their non-covalent association.

Results

Monomer-dimer equilibrium of UptA. We expressed *B. subtilis* UptA in *E. coli* and introduced the purified protein into the mass spectrometer from a buffer containing 0.05% LDAO and 200 mM ammonium acetate (pH 8.0). The mass spectrum of UptA displays two charge state distributions

assigned to monomers (22963.49±0.70 Da) and dimers (45925.21±0.65 Da) (Fig. 1B). To confirm the non-covalent association of UptA monomers, we isolated the 9+ charge state assigned to the dimer and subjected these ions to high-energy collisional dissociation (HCD, Fig. 1C). The resulting MS^2 spectrum displays new peaks that correspond by mass to UptA protomers, and bear charges complementary to the isolated parent ions (+5 and +4) (Fig. 1D). Of note, the experimental mass for the UptA monomer is higher than the theoretical sequence mass (22936.36 Da) by 28 Da, suggesting an endogenous modification. To identify this unknown modification, we activated the monomer (6+ charge state) using HCD, yielding a plethora of *b*- and *y*-type fragment ions. The observed fragments are consistent with the formylation of the N-terminal methionine of UptA (Fig. S1). Bacterial inner membrane proteins are normally co-translationally formylated on the N-terminus, however, this modification is rarely observed *in vitro* due to subsequent removal by the cytosolic deformylase (32). Therefore, retainment of N-terminal formylation on UptA suggests periplasmic localisation of the N-terminus of UptA, thus supporting the predicted N-out topology (23). Additionally, we observe UptA in monomeric and dimeric forms in other detergents (Fig. S2), confirming the oligomeric composition of UptA, which might apply to other bacterial DedA homologues.

UptA binds C_{55}-P with high affinity. We explored the binding affinity of UptA towards C_{55}-P by recording mass spectra for solutions containing 2.5 µM UptA and 0 to 40 µM C_{55}-P in 200 mM ammonium acetate, 0.05% LDAO at pH 8.0. The mass spectrum for the equimolar mixture of UptA and C_{55}-P yielded peaks corresponding to UptA in its apo form and in complex with C_{55}-P (Fig. 2A), an indication of high-affinity binding interactions. Further increase in the concentration of C_{55}-P enhanced the intensity of the UptA:C_{55}-P complex, together with the emergence of additional binding events (Fig. 2A). We deconvoluted the spectra (33) to extract mean relative intensities of bound and unbound forms of UptA in the spectral series. The data reflected an increase in the relative abundance of UptA:$(C_{55}\text{-P})_n$ complexes as a function of the concentration of C_{55}-P (Fig. 2B). For the first binding event, the relative intensity plateaued at a protein/ligand molar ratio of ~4 (Fig. 2B). By fitting the experimentally observed intensity ratios to the Hill equation, we obtained an apparent K_d = 5.7 µM (95% CI: 5.0 to 6.4 µM) for the binding of one C_{55}-P molecule to UptA. This K_d value for UptA/C_{55}-P binding is of the same order of magnitude as the binding interactions for MurG/lipid I (K_d = 1.89±0.6 µM) (34) and MurJ/lipid II (K_d = 2.9±0.6 µM) (14), indicating that UptA exhibits a similarly high affinity binding with respect to C_{55}-P.

To investigate the binding selectivity of UptA for monophosphate (C_{55}-P) versus diphosphate (C_{55}-PP) forms of the lipid carrier, we performed competitive binding assays. First, we recorded mass spectra for a mixture of UptA with increasing concentrations of C_{55}-PP. We observed peaks assigned to UptA in ligand-free and C_{55}-PP-bound forms, and the relative intensity of the UptA:C_{55}-PP complex increased with increasing concentration of C_{55}-PP (Fig. 2C). However, the

relative intensities of UptA:C_{55}-PP yielded a significantly higher apparent dissociation constant K_d = 15.3 µM (95% CI: 9.5 to 32.8 µM) than that obtained for C_{55}-P (K_d = 5.7±0.7 µM). Being within an order of magnitude, these dissociation constants suggest that UptA forms extensive contact with both forms of the lipid carriers, but that the protein interacts more favourably with C_{55}-P than C_{55}-PP. We therefore conclude that UptA is more selective towards C_{55}-P than C_{55}-PP, thus confirming its

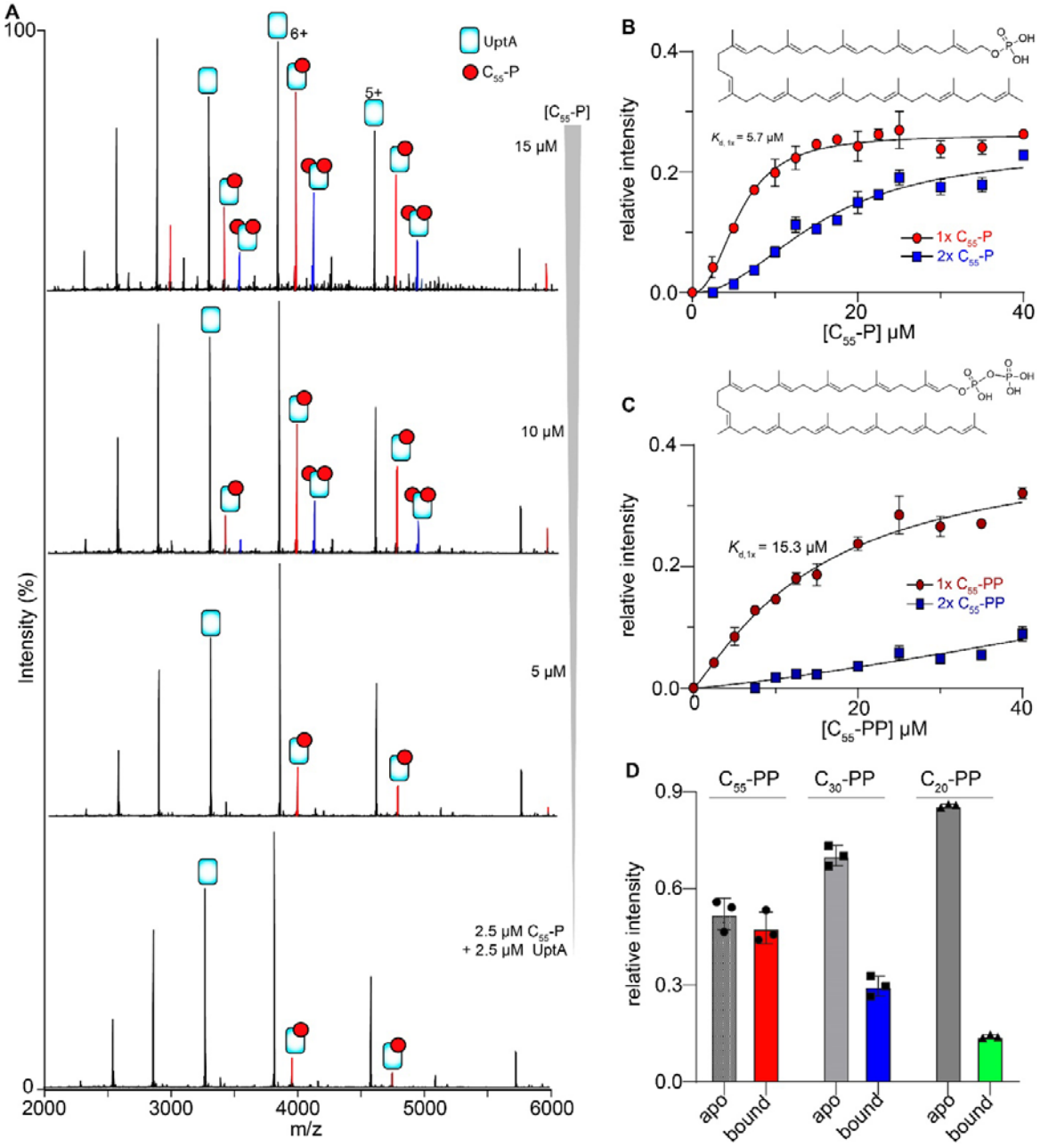

preferred endogenous substrate.

Fig 2. UptA binds C_{55}-P with a high affinity. A) Spectra for UptA incubated with different concentrations of C_{55}-P in a buffer containing 200 mM ammonium acetate (pH 8), 0.05% LDAO. **B-**

C) The relative abundance of UptA bound to one (1x) or two (2x) molecules of C_{55}-P (panel B) and C_{55}-PP (panel C). Inserts, chemical structures of C_{55}-P and C_{55}-PP. Each data point represents an average of 3 replicate measurements, and the curves represent the best fits of the data to Hill's equation (see methods), error bars are standard deviations. **D**) Mean relative intensity of ligand-free and ligand-bound UptA in spectra recorded for 4 µM UptA incubated with 40 µM C_{20}-P, 40 µM C_{30}-P, or 40 µM C_{55}-P. UptA binds the 'true' carrier lipid C_{55}-P in preference to the shorter chain analogues. Bar is the mean of three (3) independent replicates, error bars are standard deviations.

UptA interacts more favourably with C_{55}-P than its shorter-chain analogues. Next, we investigated the chain length selectivity of UptA by testing its interaction with C_{20}-P, C_{30}-P and C_{55}-P. For this experiment, we incubated 4 µM UptA with a 10-fold molar excess of C_{20}-P, C_{30}-P and C_{55}-P at pH 8.0 and recorded spectra under the same conditions. For the UptA/C_{20}-P sample, the spectrum exhibits low-intensity peaks corresponding by mass to UptA:C_{20}-P complexes, leaving most of the protein in the apo form (Fig. 2D, Fig. S3). We observed more intense protein/ligand complexes in the case of UptA/C_{30}-P, indicating a higher binding affinity of C_{30}-P compared to C_{20}-P. The spectra recorded for the UptA/C_{55}-P mixture under the same condition resolved up to four binding events per UptA molecule (Fig. S3), indicating a more favourable interaction compared to the lipidic substrate with shorter chains. Accordingly, the relative intensity of UptA in complex with C_{55}-P is higher than in the case of UptA-bound C_{30}-P and C_{20}-P (Fig. 2D, Fig. S3). Thus, the interaction of UptA with the lipid carrier is enhanced with the hydrophobic tail of C_{55}-P, supporting our hypothesis that the long polyprenyl tail of the lipid carrier forms extensive contact with UptA. Together, these data are consistent with C_{55}-P being the preferred endogenous substrate for UptA.

Amino acid residues mediating C_{55}-P interactions with UptA.

Two conserved arginine residues (R112 and R118) in the membrane re-entrant helices of UptA have been suggested to impair the cellular function of UptA by making the cells more susceptible to inhibition by amphomycin (23). Based on the model structure of UptA predicted by Alphafold, the R112 residue should engage Q64 while R118 is able to form hydrogen bonds with E32 and W146 to stabilise the intramembrane helices (Fig. 3A). To test for the impact of these residues on C_{55}-P binding, we generated the E32A, Q64A, R112A, and R118A UptA point mutants. After purification of the proteins, using the same protocol as the wild type, we equilibrated aliquots of each protein variant (5 µM) with C_{55}-P (10 µM) and recorded spectra under the same instrument settings (Fig. S4). The resulting spectra exhibited peaks consistent with C_{55}-P binding in all cases; only a modest reduction in C_{55}-P binding intensity was observed in the case of the R112A mutant compared to the wild type (Fig. 3B). We surmised that single point mutation was insufficient to attenuate binding and generated a double mutant (R112A/R118A). Comparing the C_{55}-P binding affinity of the double mutant with the wild type we found a more significant reduction in C_{55}-P binding, suggesting that

both residues are important for C_{55}-P binding. We additionally generated a double mutant R112E/R118E in which the polarity of both native arginine residues in the WT are reversed. This mutant exhibited the weakest C_{55}-P binding of all variants tested (Fig. 3B). This observation suggests that Coulombic repulsion between the glutamates and C_{55}-P destabilises binding interactions. Alternatively, impaired hydrogen bonding between R118 and EQ64 on the one hand, and R118 and E32 could also disrupt C_{55}-P binding sites. Either or both mechanisms could be at play, highlighting the critical roles of R112 and R118 in the binding of C_{55}-P to UptA.

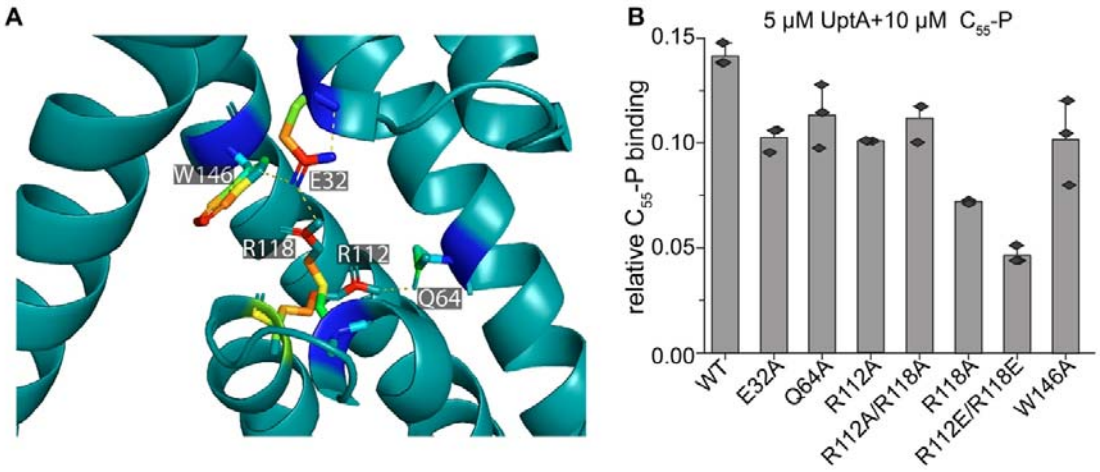

Fig. 3. Probing the amino acid residues involved in UptA-C_{55}-P binding. A. Zoomed views of UptA model structure showing hydrogen bonding networks surrounding R118 and R112. **B.** Relative intensity of C_{55}-P bound to UptA wild type and mutants. Bars represent the mean of three biological replicates with each data point shown in black, error bars are standard deviations. The double mutant at residues R112 and R118 caused the most significant reduction in C_{55}-P binding.

C_{55}-P binding to UptA is sensitive to pH. Membrane flippases, such as MurJ, are driven by proton-motive force (35) and exhibit pH-dependency in ligand binding (14). We considered the possibility that substrate interactions of UptA might exhibit a pH dependency. To this end, we equilibrated C_{55}-P with UptA at a protein/ligand molar ratio of 1:4 in a buffer of the same composition but at a more acidic pH. The resulting spectrum exhibits peaks consistent with monomeric UptA in an apo form, and in complex with 1 and 2 molecules of C_{55}-P (Fig. S5). We also observed UptA dimer in complex with up to two C_{55}-P molecules (Fig. S5). However, the intensity of peaks assigned to ligand-bound UptA is more intense at pH 8.0 compared to pH 5.0 (Fig. 4A, Fig. S5). These results imply that more favourable interactions occur under physiologically relevant pH conditions. As a negative control, we tested for pH sensitivity of C_{55}-P binding to MraY, the latter being the downstream enzyme in the peptidoglycan pathway that couples UDP-MurNAc pentapeptide to

C_{55}-P. To this end, we equilibrated MraY and C_{55}-P at a molar ratio of 1:4 in a buffer of pH 8.0 and pH 5.0 In this case, the spectra show no significant difference in the intensity of C_{55}-P bound to MraY at pH 8.0 and at pH 5.0 (Fig. 4B, Fig. S5). We therefore conclude that environmental pH modulates the interaction of C_{55}-P with UptA, and potentially its transport mechanism.

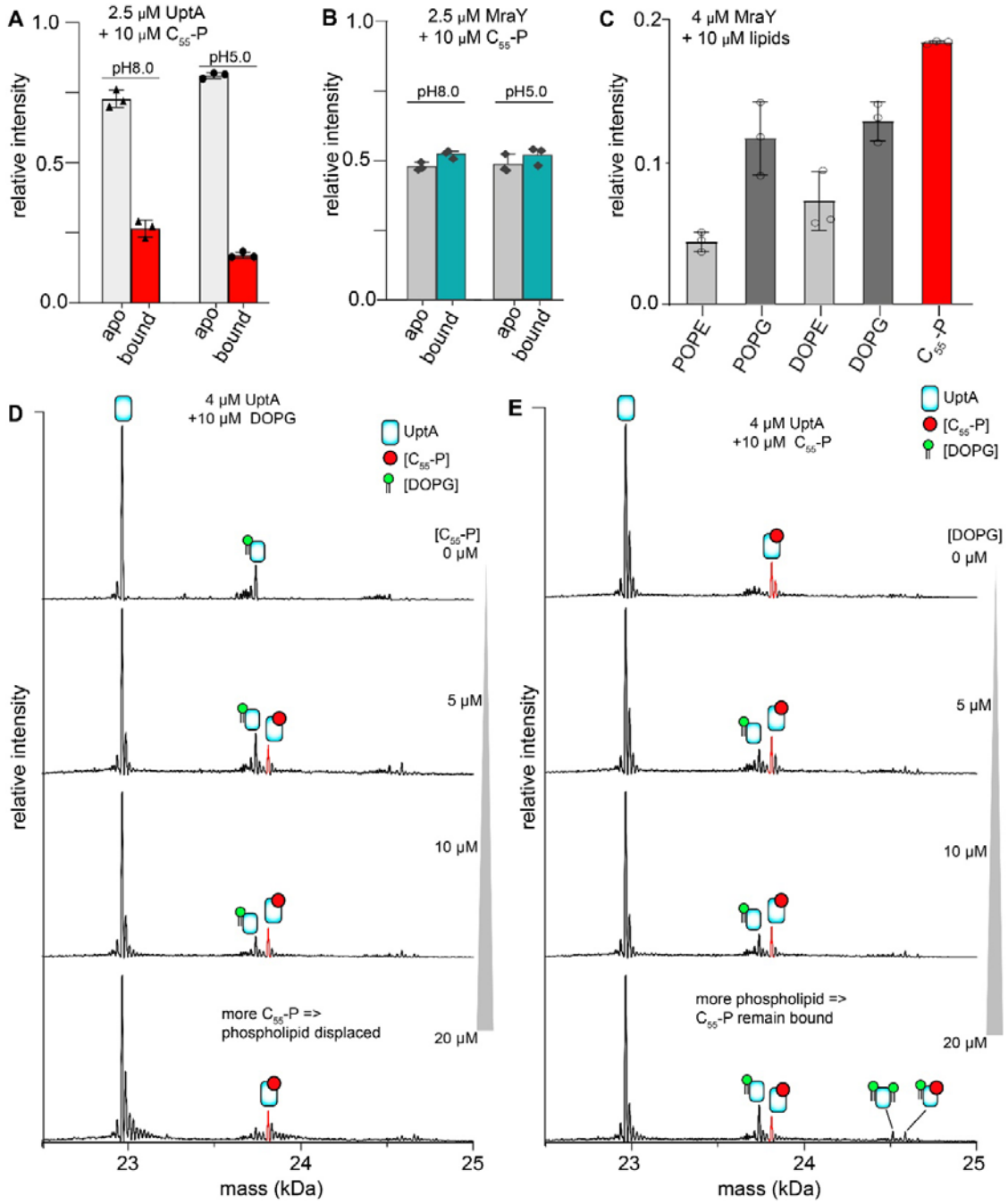

Fig 4. UptA preferentially binds C_{55}-P over membrane phospholipids. A-B) Mean relative intensity of apo and lipid-bound UptA and MraY at pH 8.0 and pH 5.0. UptA binds C_{55}-P more

favourably at pH 8 than pH 5 but MraY exhibit no pH-dependency. **C**) Mean relative intensity of lipid-bound UptA in the spectra for 4 µM UptA and 10 µM of each lipid. DOPG and POPG interact more favourably with UptA than DOPE and POPE. C_{55}-P binds to UptA more intensely than the phospholipids. Bar represents the mean of three independent replicates, data points are shown as open circles, and error bars are standard deviations. **D**) Deconvoluted mass spectra of mixtures containing 4 µM UptA,10 µM DOPG and increasing concentrations of C_{55}-P. C_{55}-P out-competes phospholipids for UptA binding. **E**) Spectra for 4 µM UptA and 10 µM C_{55}-P, then incubated with increasing concentrations of DOPG. The latter could not displace UptA-bound C_{55}-P.

C_{55}-P binds preferentially to dimeric forms of UptA. Since purified UptA displayed monomer-dimer equilibria, we considered the possibility that C_{55}-P might preferentially interact with one oligomeric species over the other. To probe this hypothesis, we used the UptA point mutant E32A since the latter consistently retained a higher dimer population than the wild type (Fig. S6). We prepared and analysed solutions containing 2.5 µM E32A UptA and 0-20 µM C_{55}-P at pH 8.0. The resulting spectra exhibited peaks assigned to UptA monomers and dimers in apo and C_{55}-P bound forms (Fig. S6). The mean relative intensity of ligand-bound dimers is however more intense than the corresponding peaks for the ligand-bound monomers (Fig. S6). Together these data indicate that the ligand C_{55}-P binds to the dimer fraction with a higher affinity than to monomers. Notably, the total monomer-dimer fraction does not change significantly in the presence of C_{55}-P, and the preferential ligand binding to the dimer fractions was observed at both pH 8.0 and pH 5.0 (Fig. S6). Together these observations suggested that dimerisation promotes ligand interactions with UptA, and potentially its cellular function.

C_{55}-P outcompetes phospholipids for UptA binding. DedA family proteins are proposed to either translocate carrier lipids, membrane phospholipids, or both. We therefore probed the interaction of UptA with membrane phospholipids to understand if the latter could modulate its function. For this purpose, we selected the anionic lipids phosphatidylglycerols (PG) and phosphatidylethanolamines (PE), being the major classes of phospholipid headgroups found in *B. subtilis* (36). We then recorded mass spectra of solutions containing 4 µM UptA incubated with 10 µM POPE, DOPE, POPG, DOPG and C_{55}-P. The resulting data shows that UptA binds to POPG and DOPG more intensely than POPE and DOPE, respectively (Fig. 4C). Together these observations suggest that UptA interacts more favourably with anionic than cationic lipids. Importantly, C_{55}-P binds to UptA with higher relative affinity than any of these diacylglycerol phospholipids (Fig. 4C), in line with C_{55}-P being its native substrate.

To investigate whether or not C_{55}-P can outcompete phospholipids in binding to UptA we incubated solutions containing UptA-DOPG with increasing concentrations of C_{55}-P. Spectra were recorded

after aliquots of the solution were equilibrated on ice for 15 mins. Notably, spectra in the absence of C_{55}-P reflected the binding of up to two molecules of DOPG per UptA (Fig. 4D). The presence of C_{55}-P caused attenuation of the intensity DOPG-bound UptA in a concentration-dependent manner. At the highest C_{55}-P concentration tested (20 µM), C_{55}-P has displaced most of DOPG from UptA (Fig. 4D). We therefore hypothesised that phospholipids should be unable to outcompete C_{55}-P bound to UptA. To test this hypothesis, we incubated UptA with C_{55}-P and then titrated in an increasing concentration of DOPG. Indeed, C_{55}-P remains bound to UptA even in the presence of excess DOPG (20 µM) (Fig. 4E), indicating that phospholipids could not displace C_{55}-P from UptA. Analogous experiments with DOPE show that C_{55}-P effectively outcompete DOPE for UptA binding but the latter could not displace C_{55}-P from UptA (Fig. S7). Together this study shows that UptA interacts more favourably with C_{55}-P than with membrane phospholipids, thereby establishing C_{55}-P as the preferred endogenous substrate.

Lipopeptide antibiotics disrupt UptA:C_{55}-P complex. We next sought to identify an antibiotic that can intercept flippase function by disrupting its interaction with the carrier lipid substrate. We tested a range of cell-wall targeting antibiotics before selecting daptomycin, amphomycin, and aspartocin, as these lipopeptides bind to UptA with a high affinity (see below). Daptomycin is known to kill bacteria by depolarising the membrane (37) and by complexing with lipid II (38). We investigated if daptomycin affects C_{55}-P binding to UptA by recording spectra for solutions containing 2.5 µM UptA, 10 µM C_{55}-P and different concentrations of daptomycin. In the absence of antibiotic, the spectrum exhibited peaks assigned to UptA in apo form, and in complex with 1 and 2 C_{55}-P molecules (Fig. 5A). In the presence of daptomycin, we observed additional peaks corresponding to the binary complex UptA:daptomycin and the ternary complex UptA:C_{55}-P:daptomycin. Further increases in daptomycin concentration resulted in higher intensity of these complexes, indicating that the antibiotic does not compete against C_{55}-P binding to UptA. The peak intensity of UptA:C_{55}-P:daptomycin ternary complex suggested that daptomycin does not compete for the same binding sites as C_{55}-P on UptA, and does not sequester C_{55}-P significantly from UptA. Accordingly, the reduction in the relative intensity of UptA:C_{55}-P complex is compensated for by the abundance of UptA: C_{55}-P:daptomycin complex. (Fig. 5A).

Amphomycin and derivatives are known to kill bacteria by forming complexes with free C_{55}-P (39), however, whether or not this involves a direct interaction with a protein cellular target is not known. We therefore investigated how amphomycin affects the UptA:C_{55}-P complex. We recorded spectra for solutions containing 2.5 µM UptA, 10 µM C_{55}-P and then equilibrated aliquots with increasing concentrations of amphomycin. The spectra exhibited peaks consistent with amphomycin binding to UptA, in addition to C_{55}-P binding. We find that the peak intensities of the UptA:C_{55}-P complex reduce with respect to an increase in the concentration of amphomycin (Fig. 5B). Compared to the

case of daptomycin, however, little-to-no UptA:C_{55}-P complexes remained in the presence of 10-fold molar excess of amphomycin (Fig. 5B). To verify these results, we performed similar experiments with aspartocin D, an analogue of amphomycin. We find that aspartocin D similarly binds to UptA and induces dissociation of UptA:C_{55}-P complex (Fig. S8). Bacitracin is a peptide antibiotic whose mode of action is to sequester C_{55}-PP thereby halting carrier lipid homeostasis (40). To test the specificity of amphomycin interaction with UptA and C_{55}-P, we prepared UptA/C_{55}-P mixtures and then equilibrated aliquots with increasing concentrations of bacitracin. In line with the specificity of bacitracin for C_{55}-PP rather than C_{55}-P, bacitracin binds to UptA only with a low intensity and does not compete against C_{55}-P, even at elevated concentrations of 200 µM (Fig. S8). Taken together, these data indicate that amphomycin and aspartocin D induce dissociation of UptA:C_{55}-P complexes, by binding directly to UptA in addition to their known propensity to form complexes with free C_{55}-P molecules (39).

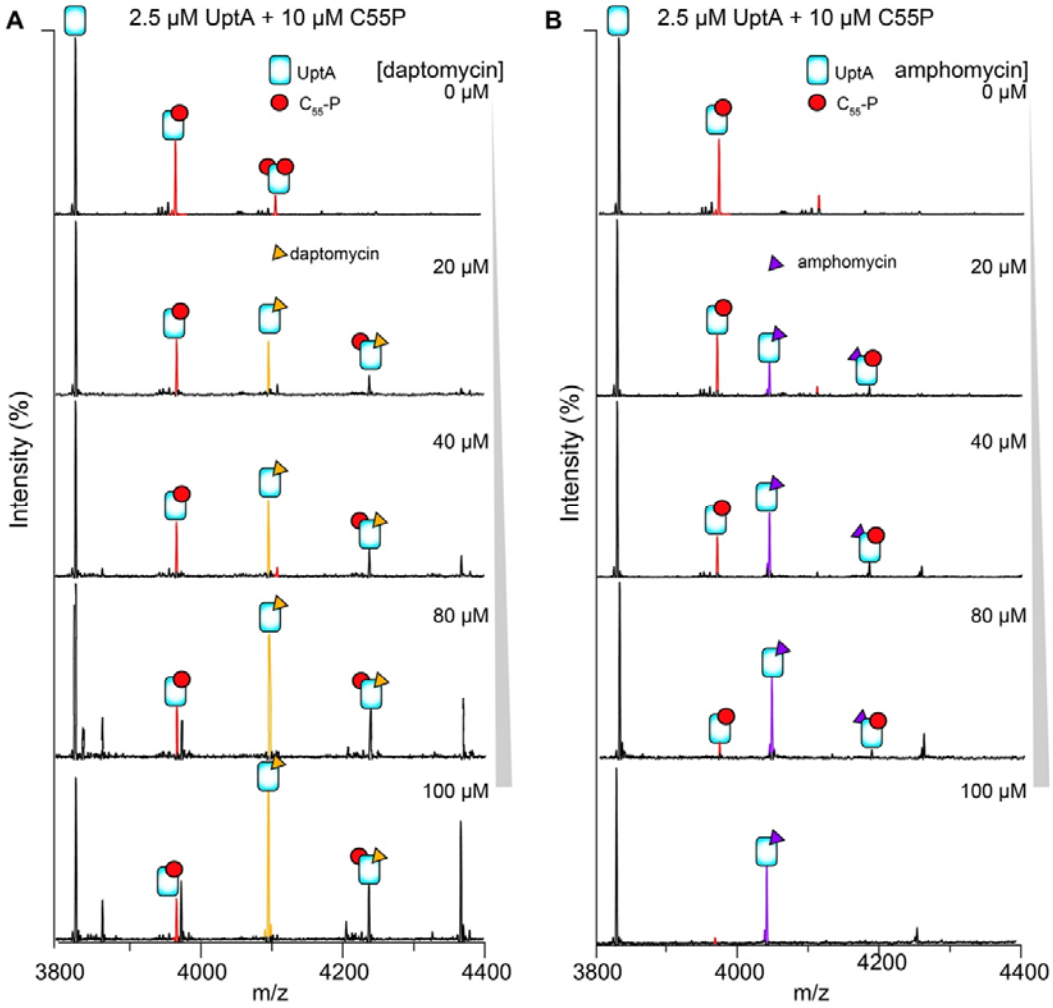

Fig. 5 UptA function can be intercepted by lipopeptide antibiotics. A) Mass spectra (6+ charge state) for solutions containing 2.5 µM UptA and 10 µM C_{55}-P incubated with 0-100 µM daptomycin.

Complexes of UptA with C_{55}-P and daptomycin are labelled. **B**) Spectra (6+ charge state) for solutions containing 2.5 µM UptA and 10 µM C_{55}-P incubated with 0-100 µM amphomycin. Amphomycin destabilises the UptA:C_{55}-P complex whereas daptomycin has a modest impact. Data are displayed as the mean of three independent replicates, and error bars are standard deviations.

Discussions

In this study, using native MS, we investigated the interplay of multiple lipidic substrates and antibiotics for UptA (summarised in Fig. 6). UptA is a representative member of the DedA family of transporters that mediate carrier lipid recycling in peptidoglycan biosynthesis. Specifically, we report that purified UptA exists as an equilibrium of monomers and dimers, suggesting that DedA proteins might form dimers in the native membrane when lateral pressures in the lipid bilayers (41) might prevent their dissociation. In line with the dependency of DedA family proteins on proton motive force (42), we found that the monomer-dimer ratio of UptA is sensitive to pH. This feature contrasts with those of the upstream peptidoglycan enzymes MraY (34, 43) and UppP (44, 45) whose dimerization are promoted by lipid binding.

Our studies also show that UptA selectively binds to C_{55}-P over C_{55}-PP and that the protein interacts more favourably with C_{55}-P than the shorter chain analogues C_{30}-P and C_{20}-P. This implies that the hydrophobic tail of C_{55}-P makes extensive contact with UptA, promoting the binding interactions and potentially facilitating the transport of carrier lipids. The higher affinity of UptA towards the monophosphate form of the carrier lipid, rather than the diphosphate form, favours a mechanism in which UptA mediates unidirectional flipping of C_{55}-P rather than acting as a scramblase for both C_{55}-P and C_{55}-PP. We further show that UptA interacts more favourably with the anionic lipids DOPG and POPG than the cationic lipids DOPE and POPE and that these lipids are readily displaced by C_{55}-P. This binding preference agrees with UptA being responsible for C_{55}-P rather than the phospholipid translocation (23). Competition between anionic lipids, which are more abundant in the native lipid bilayer than C_{55}-P, suggests that both lipids bind near the same sites on UptA and that the local lipid environment of UptA can potentially modulate its cellular function. We observed less C_{55}-P binding to UptA in the presence of excess H^+. This suggests that the UptA undergoes a proton-driven conformational change accompanying C_{55}-P flipping and release, similar to the proton-coupled amino acid (46) and antimicrobial peptide symporters (47).

We provided molecular-level evidence that the conserved arginine (R112 and R118) residues in the putative membrane re-entrant helices of UptA are important for its substrate binding interactions, confirming earlier reports that *B. subtilis* strains bearing these mutations on UptA are more susceptible to inhibition by MX2401, a derivative of amphomycin (23). We further showed that amphomycin and daptomycin bind with high affinity to UptA. Accordingly, the chemical scaffolds of these lipopeptides can therefore inspire the development of analogues that can intercept the cellular function of UptA and thus compromise the cell wall formation.

Despite the combined cellular pool of C_{55}-PP and C_{55}-P being limited to ~1.5×10^5 molecules per cell (48), they mediate the transport of glycan-bearing components of the cell wall peptidoglycan, teichoic acid and capsular polysaccharide (49). Therefore, antibiotics that intercept C_{55}-P and its flippases are potential drug targets that can potentially intercept multiple pathways and thus mitigate drug resistance. Accordingly, C_{55}-PP is the target of bacitracin and teixobactin (50, 51). Friulimicin and amphomycin analogues intercept bacterial cell wall formation by forming complexes with C_{55}-P (23, 52-54). Herein we show that amphomycin and aspartocin D can additionally induce dissociation of the UptA: C_{55}-P complex, and bind directly to UptA, a finding that can therefore guide the development of new antibiotic analogues to intercept the flippase function of UptA and its homologues.

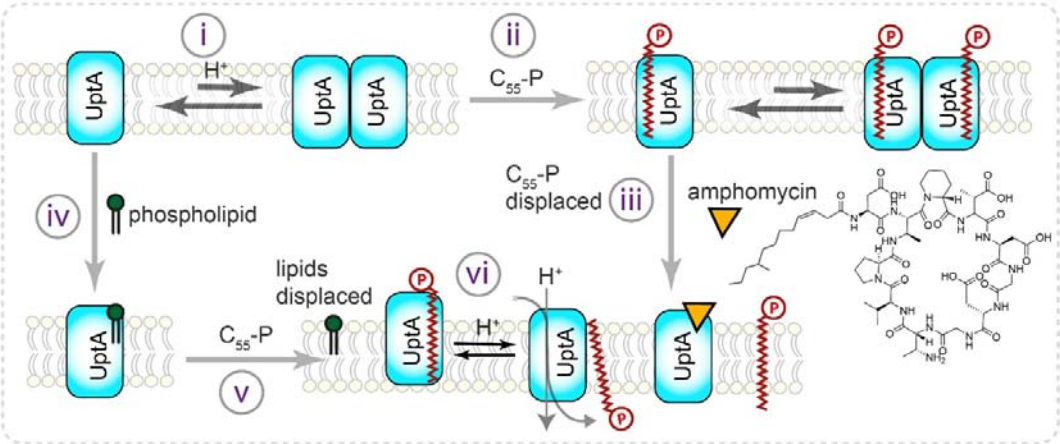

Fig. 6 Insights from native MS into the interaction of UptA with lipidic substrates and antibiotics. (i) UptA exhibits monomer-dimer equilibria, with more dimer at pH 8.0 than pH 5.0. (ii) UptA interacts with C_{55}-P more favourably than C_{55}-PP, C_{30}-P, and C_{20}-P; dimerization promotes C_{55}-P binding. (iii) Amphomycin destabilises the UptA:C_{55}-P complex, effectively out-competing the flippase for its carrier lipid substrate. (iv) UptA binds phospholipids, with a higher preference for the anionic than cationic lipids. (v) C_{55}-P is able to displace UptA-bound phospholipids, suggesting that both ligands interact with UptA near the same sites. (iv) Binding of H^+ to UptA enables translocation of C_{55}-P and its subsequent release for the next round of PG precursor synthesis.

REFERENCES

1. T. Schneider, H.-G. Sahl, An oldie but a goodie – cell wall biosynthesis as antibiotic target pathway. *International Journal of Medical Microbiology* **300**, 161-169 (2010).
2. J. M. C. Kwan, Y. Qiao, Mechanistic Insights into the Activities of Major Families of Enzymes in Bacterial Peptidoglycan Assembly and Breakdown. *ChemBioChem* **24**, e202200693 (2023).
3. A. Coleman, Y. Vohra, K. Rascati, S. Kubes, B. Moffett, Antibiotic Utilization and Efficacy Associated With Treating Pediatric Urinary Tract Infections in Texas Medicaid Patients in the First Year of Life. *Pediatr Infect Dis J* **40**, 993-996 (2021).

4. E. Sauvage, M. Terrak, Glycosyltransferases and Transpeptidases/Penicillin-Binding Proteins: Valuable Targets for New Antibacterials. *Antibiotics* **5**, 12 (2016).
5. A. J. Meeske *et al.*, MurJ and a novel lipid II flippase are required for cell wall biogenesis in Bacillus subtilis. *Proc Natl Acad Sci U S A* **112**, 6437-6442 (2015).
6. A. C. Y. Kuk, A. Hao, S. Y. Lee, Structure and Mechanism of the Lipid Flippase MurJ. *Annu Rev Biochem* **91**, 705-729 (2022).
7. S. Kumar, A. Mollo, D. Kahne, N. Ruiz, The Bacterial Cell Wall: From Lipid II Flipping to Polymerization. *Chem Rev* **122**, 8884-8910 (2022).
8. M.-C. Lo *et al.*, A New Mechanism of Action Proposed for Ramoplanin. *Journal of the American Chemical Society* **122**, 3540-3541 (2000).
9. X. Fang *et al.*, The mechanism of action of ramoplanin and enduracidin. *Molecular BioSystems* **2**, 69-76 (2006).
10. H. Barreteau *et al.*, Cytoplasmic steps of peptidoglycan biosynthesis. *FEMS Microbiology Reviews* **32**, 168-207 (2008).
11. B. C. Chung *et al.*, Crystal structure of MraY, an essential membrane enzyme for bacterial cell wall synthesis. *Science* **341**, 1012-1016 (2013).
12. A. Bouhss, A. E. Trunkfield, T. D. Bugg, D. Mengin-Lecreulx, The biosynthesis of peptidoglycan lipid-linked intermediates. *FEMS microbiology reviews* **32**, 208-233 (2007).
13. S. Ha, D. Walker, Y. Shi, S. Walker, The 1.9 A crystal structure of Escherichia coli MurG, a membrane-associated glycosyltransferase involved in peptidoglycan biosynthesis. *Protein Sci* **9**, 1045-1052 (2000).
14. J. R. Bolla *et al.*, Direct observation of the influence of cardiolipin and antibiotics on lipid II binding to MurJ. *Nat Chem* **10**, 363-371 (2018).
15. S. Kumar, A. Mollo, D. Kahne, N. Ruiz, The bacterial cell wall: from lipid II flipping to polymerization. *Chemical Reviews* **122**, 8884-8910 (2022).
16. K. Bupp, J. van Heijenoort, The final step of peptidoglycan subunit assembly in Escherichia coli occurs in the cytoplasm. *J Bacteriol* **175**, 1841-1843 (1993).
17. A. J. F. Egan, J. Errington, W. Vollmer, Regulation of peptidoglycan synthesis and remodelling. *Nat Rev Microbiol* **18**, 446-460 (2020).
18. V. M. Hernández-Rocamora *et al.*, Real-time monitoring of peptidoglycan synthesis by membrane-reconstituted penicillin-binding proteins. *eLife* **10**, e61525 (2021).
19. Y. Park, A. Taguchi, V. Baidin, D. Kahne, S. Walker, A Time-Resolved FRET Assay Identifies a Small Molecule that Inhibits the Essential Bacterial Cell Wall Polymerase FtsW. *Angewandte Chemie International Edition* **62**, e202301522 (2023).
20. M. El Ghachi, A. Bouhss, D. Blanot, D. Mengin-Lecreulx, The bacA gene of Escherichia coli encodes an undecaprenyl pyrophosphate phosphatase activity. *J Biol Chem* **279**, 30106-30113 (2004).
21. M. El Ghachi, A. Derbise, A. Bouhss, D. Mengin-Lecreulx, Identification of multiple genes encoding membrane proteins with undecaprenyl pyrophosphate phosphatase (UppP) activity in Escherichia coli. *J Biol Chem* **280**, 18689-18695 (2005).
22. R. Bernard, M. El Ghachi, D. Mengin-Lecreulx, M. Chippaux, F. Denizot, BcrC from Bacillus subtilis acts as an undecaprenyl pyrophosphate phosphatase in bacitracin resistance. *J Biol Chem* **280**, 28852-28857 (2005).
23. I. J. Roney, D. Z. Rudner, Two broadly conserved families of polyprenyl-phosphate transporters. *Nature* **613**, 729-734 (2023).
24. B. Sit *et al.*, Undecaprenyl phosphate translocases confer conditional microbial fitness. *Nature* **613**, 721-728 (2023).

25. W. T. Doerrler, R. Sikdar, S. Kumar, L. A. Boughner, New Functions for the Ancient DedA Membrane Protein Family. *Journal of Bacteriology* **195**, 3-11 (2013).
26. P. R. Panta, W. T. Doerrler, A Burkholderia thailandensis DedA Family Membrane Protein Is Required for Proton Motive Force Dependent Lipid A Modification. *Frontiers in Microbiology* **11** (2021).
27. S. Kumar, W. T. Doerrler, Members of the conserved DedA family are likely membrane transporters and are required for drug resistance in Escherichia coli. *Antimicrob Agents Chemother* **58**, 923-930 (2014).
28. I. J. Roney, D. Z. Rudner, The DedA superfamily member PetA is required for the transbilayer distribution of phosphatidylethanolamine in bacterial membranes. *Proceedings of the National Academy of Sciences* **120**, e2301979120 (2023).
29. A. Galinier, C. Delan-Forino, E. Foulquier, H. Lakhal, F. Pompeo, Recent Advances in Peptidoglycan Synthesis and Regulation in Bacteria. *Biomolecules* **13**, 720 (2023).
30. F. T. Liang *et al.*, BB0250 of Borrelia burgdorferi is a conserved and essential inner membrane protein required for cell division. *J Bacteriol* **192**, 6105-6115 (2010).
31. J. Jumper *et al.*, Highly accurate protein structure prediction with AlphaFold. *Nature* **596**, 583-589 (2021).
32. A. Ranjan, E. Mercier, A. Bhatt, W. Wintermeyer, Signal recognition particle prevents N-terminal processing of bacterial membrane proteins. *Nature Communications* **8**, 15562 (2017).
33. M. T. Marty *et al.*, Bayesian deconvolution of mass and ion mobility spectra: from binary interactions to polydisperse ensembles. *Anal Chem* **87**, 4370-4376 (2015).
34. A. O. Oluwole *et al.*, Peptidoglycan biosynthesis is driven by lipid transfer along enzyme-substrate affinity gradients. *Nature Communications* **13**, 2278 (2022).
35. F. A. Rubino, S. Kumar, N. Ruiz, S. Walker, D. E. Kahne, Membrane Potential Is Required for MurJ Function. *Journal of the American Chemical Society* **140**, 4481-4484 (2018).
36. J. A. den Kamp, I. Redai, L. L. van Deenen, Phospholipid composition of Bacillus subtilis. *J Bacteriol* **99**, 298-303 (1969).
37. W. R. Miller, A. S. Bayer, C. A. Arias, Mechanism of action and resistance to daptomycin in Staphylococcus aureus and enterococci. *Cold Spring Harbor perspectives in medicine* **6** (2016).
38. F. Grein *et al.*, Ca2+-Daptomycin targets cell wall biosynthesis by forming a tripartite complex with undecaprenyl-coupled intermediates and membrane lipids. *Nature Communications* **11**, 1455 (2020).
39. T. M. Wood *et al.*, Mechanistic insights into the C 55-P targeting lipopeptide antibiotics revealed by structure–activity studies and high-resolution crystal structures. *Chemical Science* **13**, 2985-2991 (2022).
40. J. Smith, E. Weinberg, Mechanisms of antibacterial action of bacitracin. *Microbiology* **28**, 559-569 (1962).
41. R. S. Cantor, Lateral pressures in cell membranes: a mechanism for modulation of protein function. *The journal of physical chemistry B* **101**, 1723-1725 (1997).
42. P. R. Panta, W. T. Doerrler, A Burkholderia thailandensis DedA family membrane protein is required for proton motive force dependent lipid a modification. *Frontiers in Microbiology* **11**, 618389 (2021).
43. E. Henrich *et al.*, Lipid Requirements for the Enzymatic Activity of MraY Translocases and in Vitro Reconstitution of the Lipid II Synthesis Pathway. *J Biol Chem* **291**, 2535-2546 (2016).

44. S. D. Workman, L. J. Worrall, N. C. J. Strynadka, Crystal structure of an intramembranal phosphatase central to bacterial cell-wall peptidoglycan biosynthesis and lipid recycling. *Nature Communications* **9**, 1159 (2018).
45. A. O. Oluwole *et al.*, Real-time biosynthetic reaction monitoring informs the mechanism of action of antibiotics. *J. Am. Chem. Soc.* **146**, 7007-7017 (2024).
46. M. Löbel *et al.*, Structural basis for proton coupled cystine transport by cystinosin. *Nature Communications* **13**, 4845 (2022).
47. D. Ghilarov *et al.*, Molecular mechanism of SbmA, a promiscuous transporter exploited by antimicrobial peptides. *Science Advances* **7**, eabj5363 (2021).
48. H. Barreteau *et al.*, Quantitative high-performance liquid chromatography analysis of the pool levels of undecaprenyl phosphate and its derivatives in bacterial membranes. *J Chromatogr B Analyt Technol Biomed Life Sci* **877**, 213-220 (2009).
49. M. Rausch *et al.*, Coordination of capsule assembly and cell wall biosynthesis in Staphylococcus aureus. *Nat Commun* **10**, 1404 (2019).
50. L. L. Ling *et al.*, A new antibiotic kills pathogens without detectable resistance. *Nature* **517**, 455-459 (2015).
51. R. Shukla *et al.*, Teixobactin kills bacteria by a two-pronged attack on the cell envelope. *Nature* **608**, 390-396 (2022).
52. T. M. Wood *et al.*, Mechanistic insights into the C55-P targeting lipopeptide antibiotics revealed by structure–activity studies and high-resolution crystal structures. *Chemical Science* **13**, 2985-2991 (2022).
53. T. Schneider *et al.*, The lipopeptide antibiotic Friulimicin B inhibits cell wall biosynthesis through complex formation with bactoprenol phosphate. *Antimicrob Agents Chemother* **53**, 1610-1618 (2009).
54. Z. Wang, B. Koirala, Y. Hernandez, M. Zimmerman, S. F. Brady, Bioinformatic prospecting and synthesis of a bifunctional lipopeptide antibiotic that evades resistance. *Science* **376**, 991-996 (2022).

Supporting information

Lipopeptide antibiotics disrupt interactions of undecaprenyl phosphate with UptA

Abraham O. Oluwole[1,2*], Neha Kalmankar[1,2], Michela Guida[2,3], Jack L. Bennett[1,2], Giovanna Poce[3], Jani R. Bolla[2,4] Carol V. Robinson[1,2*]

[1]Department of Chemistry, University of Oxford, South Parks Road, Oxford, OX1 3QZ, UK. [2]The Kavli Institute for Nanoscience Discovery, Oxford, South Parks Road, Oxford, OX1 3QU, UK. [3]Department of Chemistry and Technologies of Drug, Sapienza University of Rome, 00185 Rome, Italy. [4]Department of Biology, University of Oxford, South Parks Road, Oxford, OX1 3RB, UK.

Email: abraham.oluwole@chem.ox.ac.uk; carol.robinson@chem.ox.ac.uk

Table of Contents

Methods 2
Chemicals 2
Plasmids 2
Table S1: Oligonucleotides using to generate plasmids for the expression of UptA mutants 2
Expression and purification of UptA 2
Sample preparation for native MS 3
Native mass spectrometry 4
Supplementary Figures 5
Fig. S2. Oligomeric state of UptA in different detergents. 6
Fig. S3. UptA binds carrier lipids of longer chain lengths more intensely than those of shorter chain. 7
Fig. S4. Native MS analysis of C_{55}-P binding to UptA mutants. 8
Fig. S5. UptA binds C_{55}-P more favourably at pH 8 than pH 5. 9
Fig. S6. Dimer fraction of UptA bind C_{55}-P more than the monomeric form 10
Fig. S7. Competition for UptA between DOPE and C_{55}-P. 11
Fig. S8. Aspartocin binds to UptA and disrupts UptA:C_{55}-P interactions. 12

Methods

Chemicals

C_{55}-PP, C_{55}-P, C_{30}-P and C_{20}-P were purchased from Larodan. Phospholipids – POPE, DOPE, POPG, DOPG – were purchased from Avanti Polar Lipids. Amphomycin and aspartocin D were purchased from Cayman; while Daptomycin and bacitracin were purchased from Merck. *n*-dodecyl-*β*-D-maltoside (DDM), *n*-decyl-*β*-D-maltoside (DDM), n-octylglucoside (OG) and *n*-dodecyl-*N,N*-dimethylamine-*N*-oxide (LDAO) were from Anatrace.

Plasmids

A codon-optimised version of *Bacillus subtilis* UptA (yngC) (Integrated DNA Technologies) was inserted into a modified pET15b vector between NdeI and NheI endonuclease restriction sites by In-Fusion HD cloning kit (Takara Bio). The resulting plasmid encodes UptA fused to GFP-His_6 on the C-terminus via a TEV-protease cleavable site. Plasmids for UptA mutants were generated by site directed mutagenesis with CloneAmp HiFi PCR Premix (Takara Bio) using pairs of oligonucleotides listed in Table S1. The plasmid pET26-MBP-MraYaa bearing HRV3C protease cleavage site between the MBP and the wild-type MraY was a kind gift from S-Y Lee (Addgene plasmid #100166) (1). MraY was expressed and purified as previously described (2).

Table S1: Oligonucleotides using to generate plasmids for the expression of UptA mutants.

Primers	Sequence
E32AF	TCCAAGCGCAATTGTATTGGCCTACGGTGG
E32AR	ACAATTGCGCTTGGAATAATTTCAATCATCAGT
Q64AF	GATCGCCGCAATTTTCATTTACTGGATTGGCCGT
Q64AR	AAAATTGCGGCGATCGTTCCCCCGATA
R112AF	TTCTGCTGCCTTCATCCCTGTAGTCCGTCATGC
R112AR	ATGAAGGCAGCAGAAAACACAACCCCCG
R118AF	TGTAGTCGCACATGCTATTTCGATCCCAGCCG
W146AF	CATTCCTGCCTCCATCCTGTTCGTTTACCTGG
W146AR	ATGGAGGCAGGAATGATGGCAAGTACTGTC
R112A/R118A_Fwd	TTCTGCTGCCTTCATCCCTGTAGTCGCACATGCTATTTCGATCCCAGCCG
R112A/R118A_Rev	GCATGTGCGACTACAGGGATGAAGGCAGCAGAAAACACAACCCCCG
R112E/R118E_Fwd	ATTCATCCCTGTAGTCGAACATGCTATTTCGATCCCAGCCG
R112E/R118E_Rev	ACTACAGGGATGAATTCAGCAGAAAACACAACCCCCG

Expression and purification of UptA

Plasmids were used to transform chemically competent *E. coli* C43(DE3) cells (Lucigen) and selected on LB/Agar containing 100 µg/ml ampicillin at 37 °C. Single colonies were used to inoculate 60 mL LB containing 100 µg/ml ampicillin and were grown at 37 °C overnight for 16 h. For large-scale protein

57 expression, 10 mL of the overnight culture was aseptically transferred into 1 L of LB/ampicillin and
58 cells were allowed to grow at 37°C until the $OD_{600\ nm}$ reached 0.6-0.8 after which the temperature was
59 lowered to 18 °C. Expression of UptA-GFP was induced by adding isopropyl-β-D-
60 thiogalactopyranoside (IPTG) at a final concentration of 0.5 mM UptA-GFP and shaking for 20 h at
61 18 °C. Cells were harvested by centrifugation at 5000 × *g* and lysed immediately or stored at -80 ° C
62 until required.
63 Cells were thawed on ice and resuspended in a buffer containing 50 mM Tris-HCl (pH 7.4), 200 mM
64 NaCl, 10 µg/mL deoxyribonuclease I (DNAse I), 5 mM $MgCl_2$, 5 mM β-mercaptoethanol and EDTA-
65 free protease inhibitor cocktail tablets. The cells were then disrupted with a microfluidiser
66 (Microfluidics) operated at 20,000 psi. Non-lysed cells and debris were pelleted by centrifugation at
67 20,000 × *g* for 20 min and the clarified lysate was retained. The membranes fraction was then pelleted
68 by ultracentrifugation at 100,000 x g for 1 h. They were resuspended in a buffer containing 20 mM
69 Tris-HCl (pH 8.0), 300 mM NaCl, 20% glycerol. Membrane aliquots were either solubilised
70 immediately or flash-frozen in liquid nitrogen and stored at -80°C. The membrane was solubilised by
71 incubation with DDM at a final concentration of 1% (w/v) for 60 min. Non-solubilised aggregates were
72 removed by centrifugation at 20,000×g for 20 min and the supernatant was loaded onto a 5-ml HisTrap
73 HP column preequilibrated in buffer A (20 mM Tris-HCl (pH 8.0), 200 mM NaCl, 10% glycerol, 0.03%
74 DDM and 20 mM imidazole). After binding of the His-tagged protein, the column was washed with
75 100 mL of buffer A, and then with 50 mL of buffer B (20 mM Tris-HCl (pH 8.0), 200 mM NaCl, 10%
76 glycerol, 0.03% DDM and 100 mM imidazole). UptA-GFP was eluted from the column with buffer C
77 (20 mM Tris-HCl (pH 8.0), 200 mM NaCl, 10% glycerol, 0.02% DDM and 300 mM imidazole). To
78 remove imidazole and to cleave the GFP fusion, eluted protein was mixed with TEV protease and
79 dialysed against buffer D (20 mM Tris-HCl (pH 8.0), 150 mM NaCl, 10% glycerol, 0.02% DDM) at 4°C
80 for 16 h.
81 The digestion mixture was subsequently incubated with 2-mL bed volume of nickel nitriloacetic acid
82 (NTA) agarose resin to remove His-tagged GFP and TEV protease. Tag-free UptA was collected as
83 the flowthrough, concentrated using an Amicon centrifugal concentrator with nominal molecular
84 weight cut-off 50 kDa. The protein was finally purified by size-exclusion chromatography (SEC) using
85 a 24-mL Superdex 200 Increase column. The SEC buffer was 20 mM Tris-HCl (pH 8.0), 200 mM
86 NaCl, 0.02% DDM. UptA was concentrated to ~200 uM, aliquoted, flash-frozen flash in liquid nitrogen,
87 and stored at -80 °C until use. Concentration was measured using a Biomate UV spectrophotometer
88 at 280 nm using extinction coefficients calculated from their predicted amino acid sequences. UptA
89 mutants were purified in 3 biological replicates, using the same procedures as for the wild-type.

90 **Sample preparation for native MS**

91 Prior to measurement, the protein was buffer-exchanged into 0.05% LDAO, 200 mM ammonium
92 acetate ("MS buffer") at desired pH in using a centrifugal buffer exchange device (Micro Bio-Spin 6,
93 Bio-Rad). Stock solutions of lipids were prepared from chloroform/methanol solution by evaporating

aliquots of known volume in a SpeedVac. After drying, the lipid films were weighed and resuspended to a final concentration of 0.5 mM in 200 mM ammonium acetate (pH8) and 0.05% LDAO by vertexing. Amphomycin and aspartocin D were purchased from Cayman while Daptomycin and bacitracin were purchased from Merck. Stock solutions of 0.5 mM amphomycin, aspartocin D, daptomycin and bacitracin, were made in the same buffer. All experiments were repeated three times from newly prepared stock solutions.

Native mass spectrometry

About 3 µL protein aliquot was transferred into a gold-coated borosilicate capillary (Harvard Apparatus) and was mounted on the nano ESI source of a Q-Exactive hybrid quadrupole-Orbitrap mass spectrometer (Thermo Fisher Scientific, Bremen, Germany). The instrument settings were 1.2 kV capillary voltage, S-lens RF 200%, argon UHV pressure 3.3×10^{-10} mbar, the capillary temperature was set to 200 °C, and resolution of the instrument was set to 17,500 at a transient time of 64 ms. Voltages of the ion transfer optics –injection flatapole, inter-flatapole lens, bent flatapole, and transfer multipole were set to 5, 3, 2, and 30 V respectively. The noise level was set at 3. Unless otherwise stated, proteins were activated by applying 75 V in the high-energy collisional dissociation cell without in-source trapping. For the MS^2 spectra, parent ions were isolated using an in-source trapping voltage of -200 V, and then fragmented by applying 150-200 V in the high-energy collision-induced dissociation cell. To identify endogenous modifications using native top-down mass spectrometry, the 6+ charge state of monomeric UptA was isolated (3828 ± 5 Th) and activated using HCD (200 V) with reduced trapping pressures. The resulting fragments were detected in the Orbitrap (R = 280,000 @ *m*/*z* 200), averaging ~500 transients to maximise the signal-to-noise ratio. Theoretical fragments from N-terminally formylated UptA were matched to the MS^2 spectrum (3 ppm) using TDValidator (Proteinaceous) and manual validation. Data were visualised and exported for processing using the Qual browser of Xcalibur 4.1.31.9 (Thermo Scientific). Spectral deconvolution was performed using UniDec 6.0.2 (3). Relative binding affinities were obtained from deconvoluted spectra by dividing the intensity of ligand-bound protein peaks by the sum of the intensities of ligand-bound and ligand-free protein peaks. The mean and standard deviation of these fractional binding intensities from three independent experiments were plotted against the concentrations of the ligand C_{55}-P or C_{55}-PP. To obtain the apparent dissociation constant K_d, the mean relative intensities at different concentrations were fitted globally using GraphPad Prism 10.2.0 to Eq. (1):

$$y = \frac{B_{max} x^h}{x^h + K_d^{\,h}} \qquad (1)$$

Where y is the mean relative intensity and x is the corresponding ligand concentration. B_{max} is the maximum specific binding, K_d is the apparent dissociation constant, and h is the Hill coefficient.

Supplementary Figures

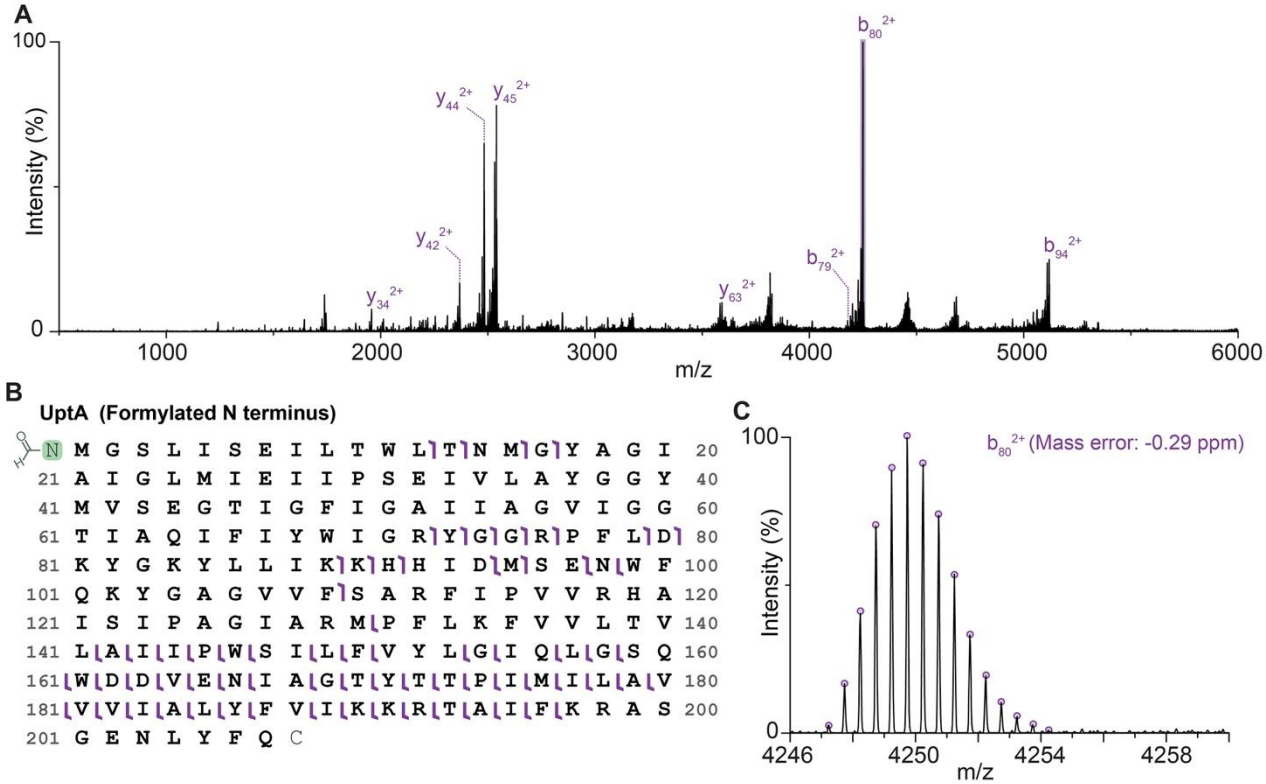

Fig. S1. UptA is formylated at the N-terminus. A. HCD MS/MS spectrum of UptA (6+). The eight most abundant assigned ions are labelled. **B**. Sequence map of the UptA construct used in this study. Terminal *b*- and *y*-type fragment ions observed in the MS/MS spectrum are indicated. **C.** Expanded view of the peak corresponding to b_{80}^{2+} ion**.** The theoretical isotopic envelope is overlaid.

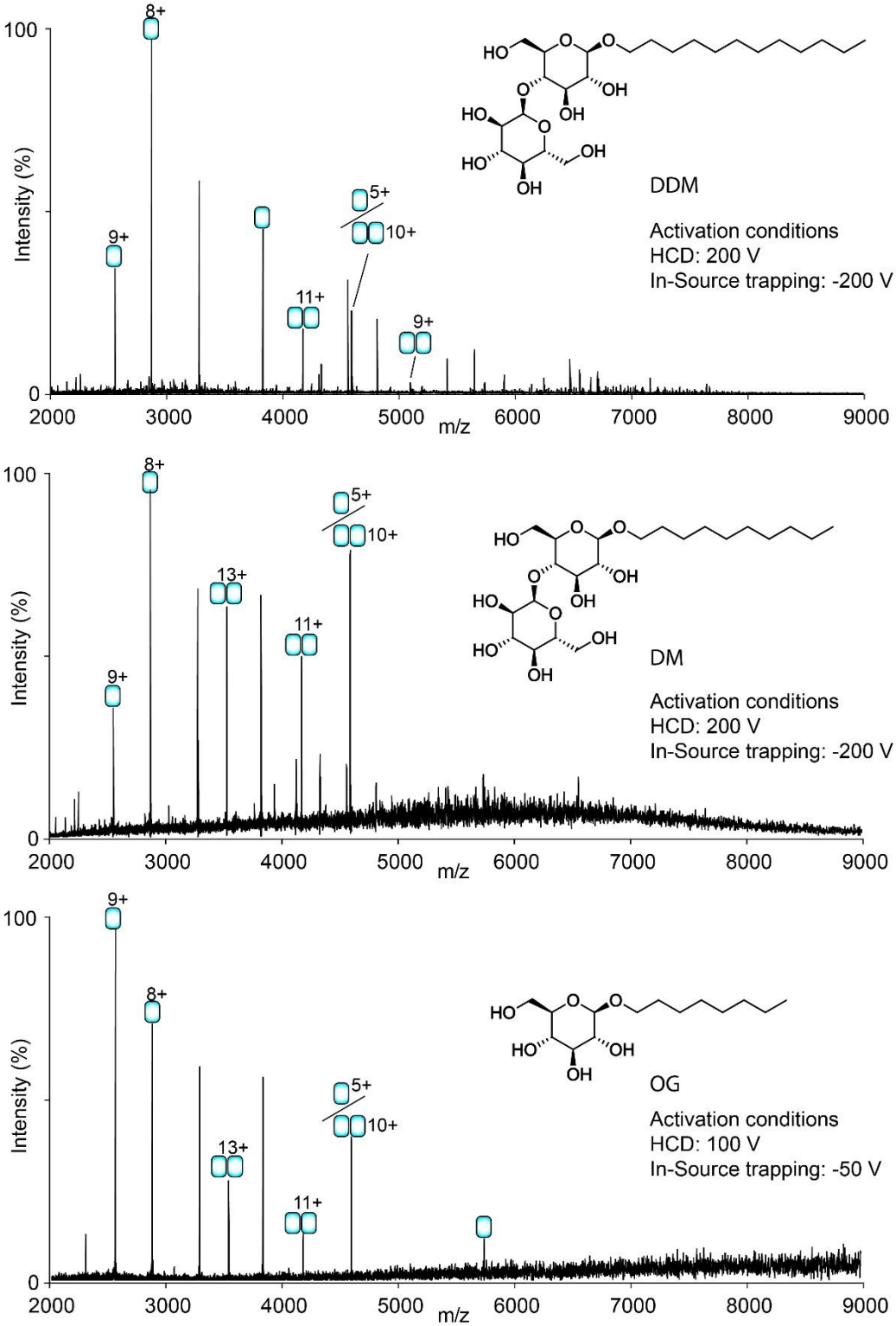

Fig. S2. Oligomeric state of UptA in different detergents. Shown are the spectra recorded for UptA in buffer containing 200 mM Ammonium acetate (pH 8.0) supplemented with indicated detergents. The instrument was tuned differently in each case to maximise the transmission of dimeric species.

142

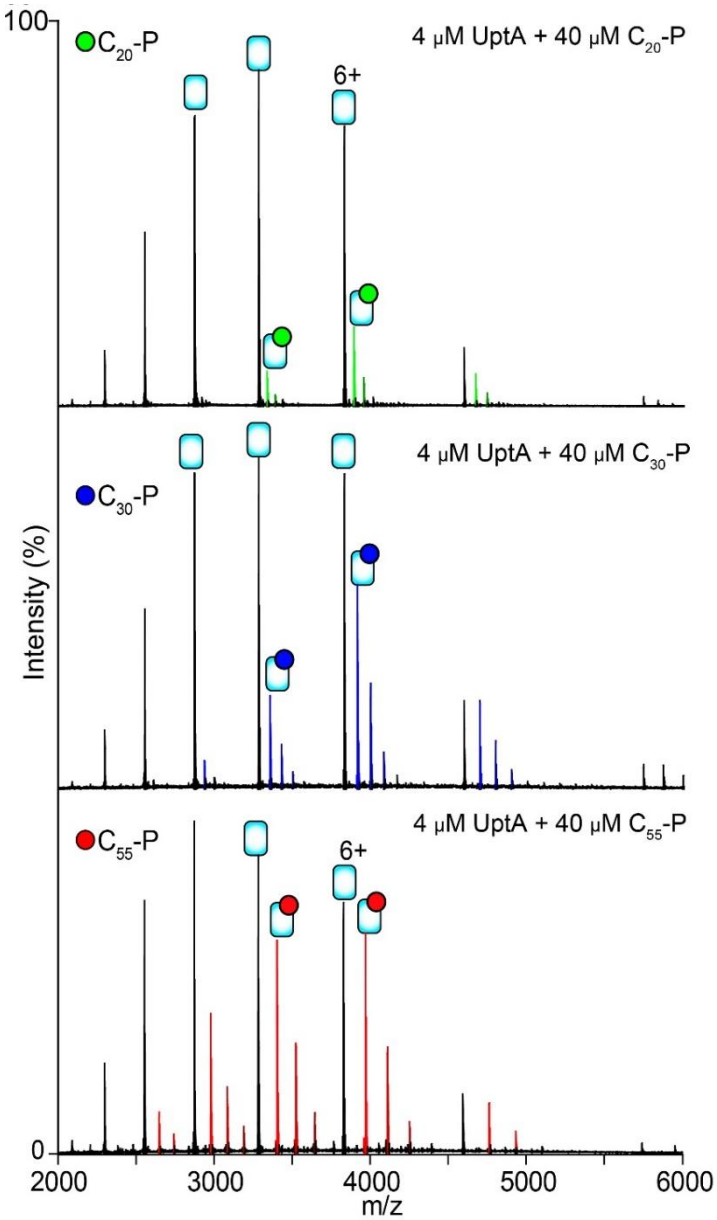

143 **Fig. S3. UptA binds carrier lipids of longer chain lengths more intensely than those of shorter**
144 **chain.** Shown are the spectra recorded for 4 μM UptA equilibrated with 10-fold molar excess of C_{20}-P,
145 C_{30}-P and C_{55}-P.

146

147

148

149

150

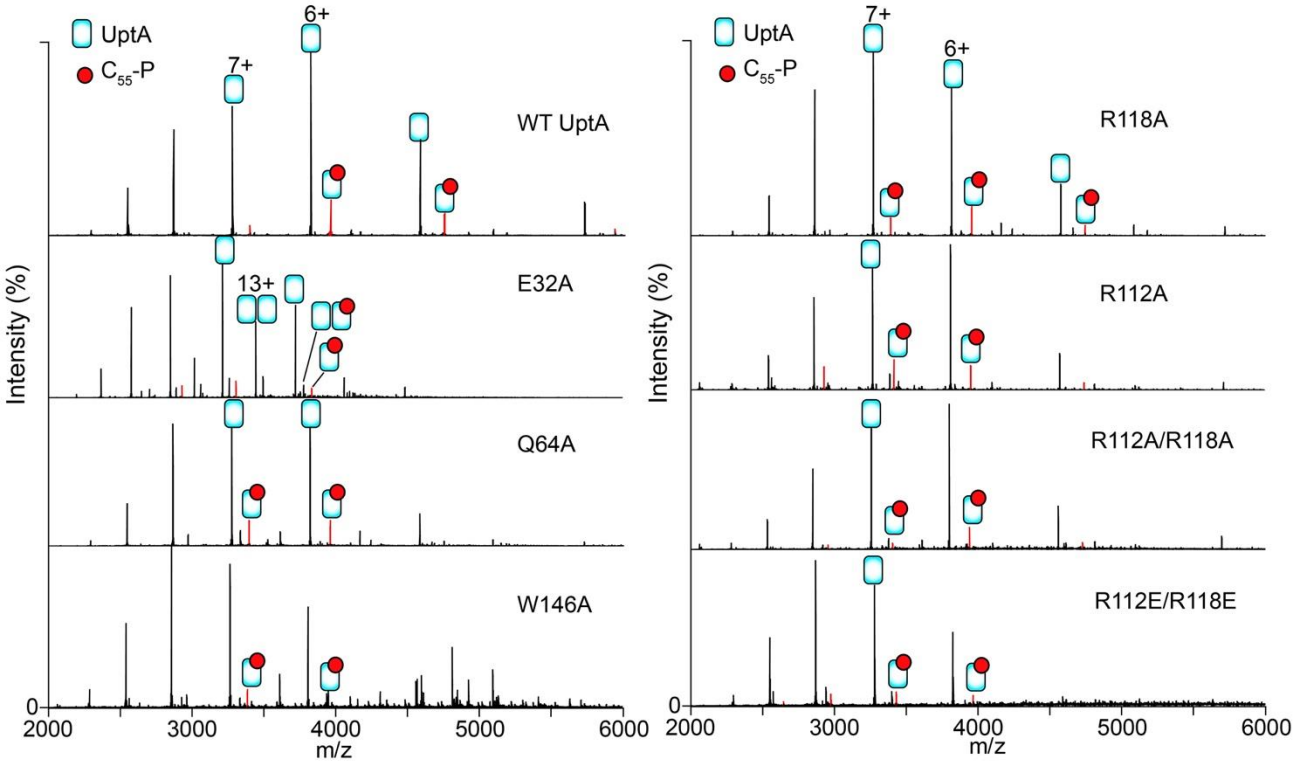

Fig. S4. Native MS analysis of C_{55}-P binding to UptA mutants. Shown are the representative spectra for UptA wild type and mutants (5 uM) incubated with C_{55}-P (10 uM). Proteins were liberated from a buffer containing 0.05% LDAO and 200 mM ammonium acetate (pH8. 02) using a collisional activation of 100 V.

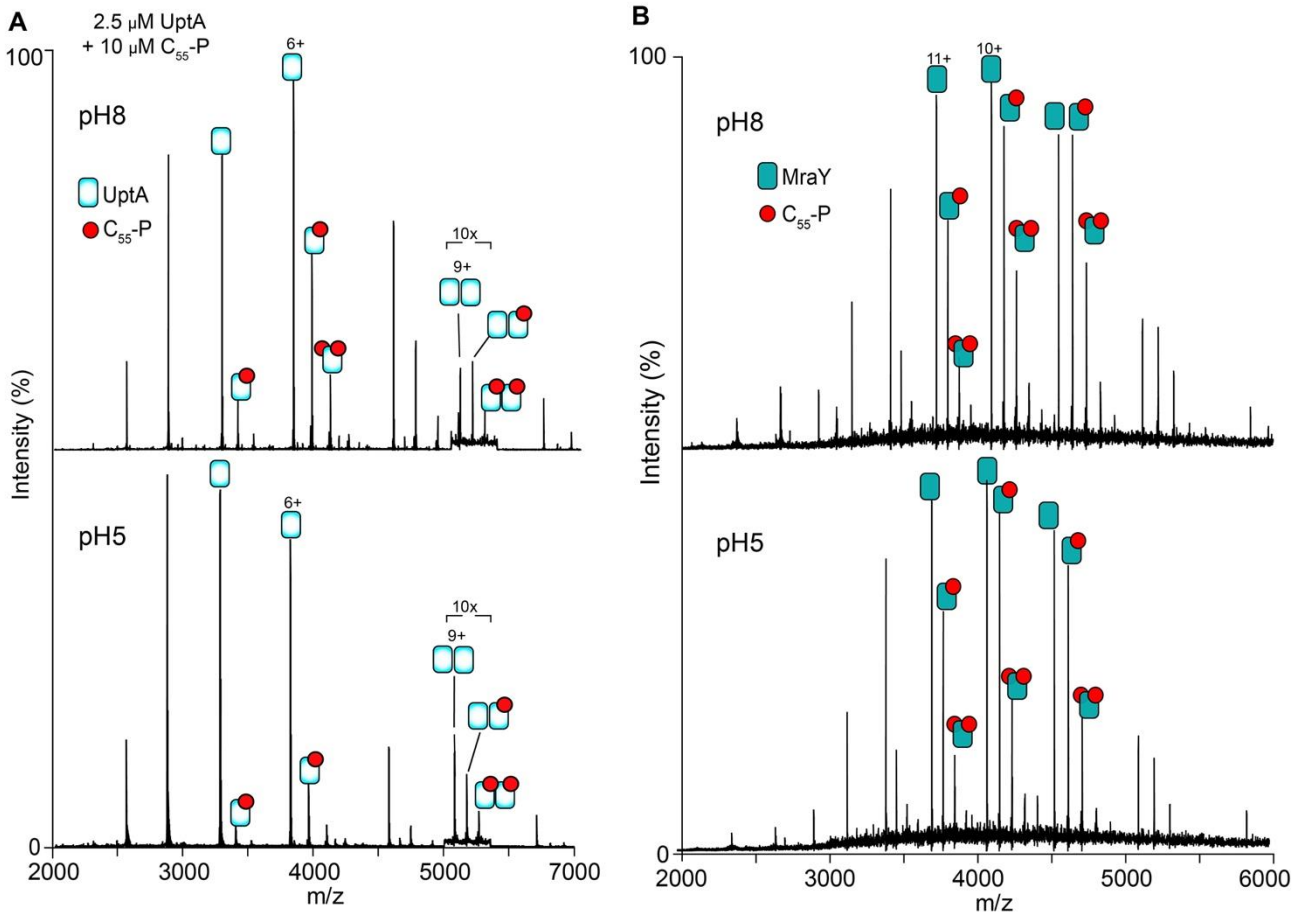

Fig. S5. UptA binds C_{55}-P more favourably at pH 8.0 than at pH 5.0. **A**. Spectra for UptA/C_{55}-P mixtures at indicated pH. Inserts, the relative abundance of apo UptA and C_{55}-P bound forms. **B.** Spectrum for MraY/C_{55}-P mixture at pH 8.0 and pH 5.0. There is no pH-dependency in C_{55}-P binding by MraY.

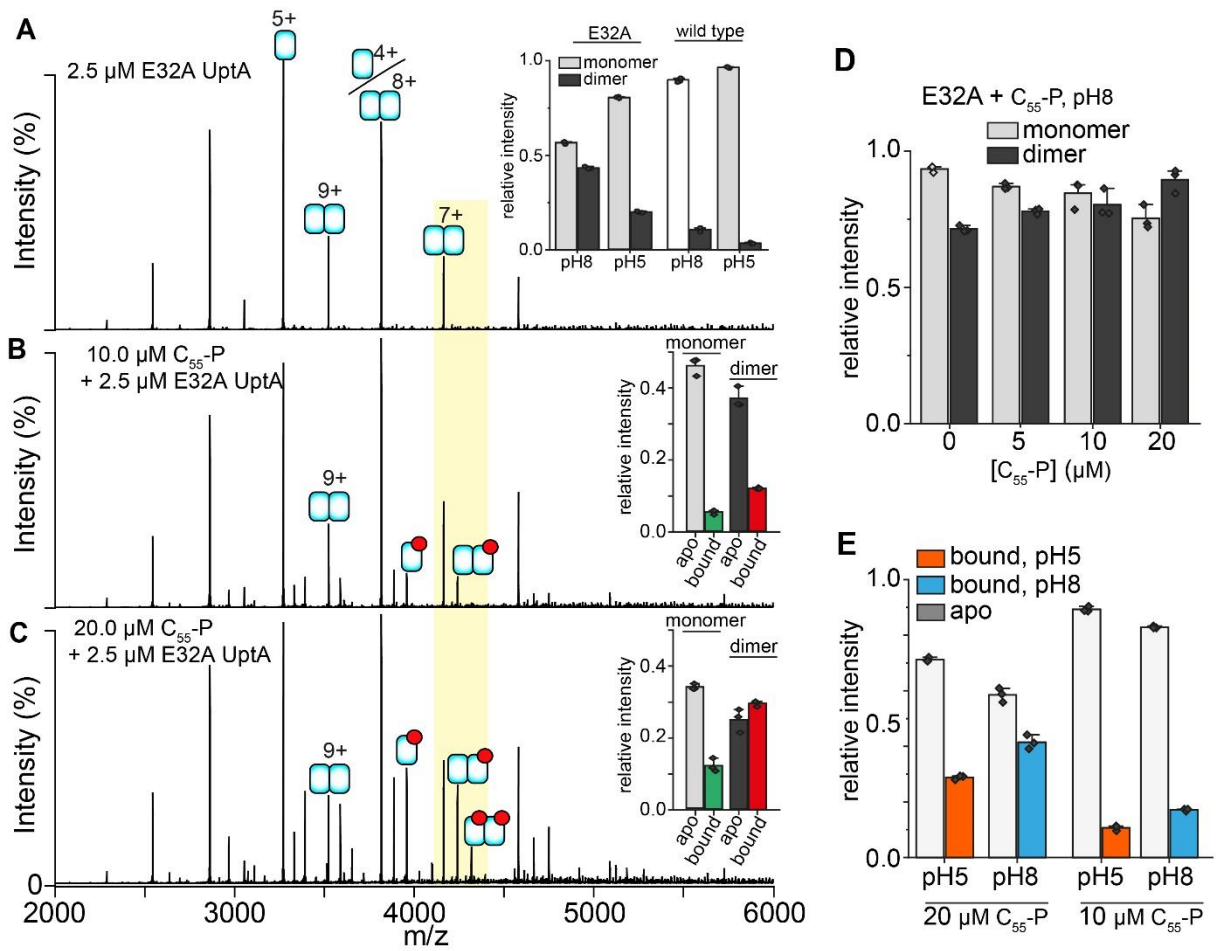

Fig. S6. Dimer fraction of UptA binds C_{55}-P more than the monomeric form. **A.** Spectra from UptA E32A mutant display peaks corresponding to monomers and dimers. Insert, the relative intensity of monomer-dimer populations in the E32A mutant and the wild-type UptA**.** More dimers are observed at pH 8.0 than at pH 5.0. **B-C.** Spectrum of UptA E32A mutant equilibrated with 10 μM and 20 μM C_{55}-P. Insert, the relative intensity of apo and C_{55}-P bound proteins in each spectrum. Dimer fractions bind the ligand more than the monomers. **D.** The total proportion of monomers and dimers in a mixture of E32A UptA and 0-20 μM C_{55}-P. The ligand C_{55}-P does not cause a significant difference in the monomer-dimer ratios. **E.** Mean relative intensity of apo and C_{55}-P bound E32A UptA at pH5 and pH8. C_{55}-P bind to UptA more intensely at pH 8.0 than at pH 5.0.

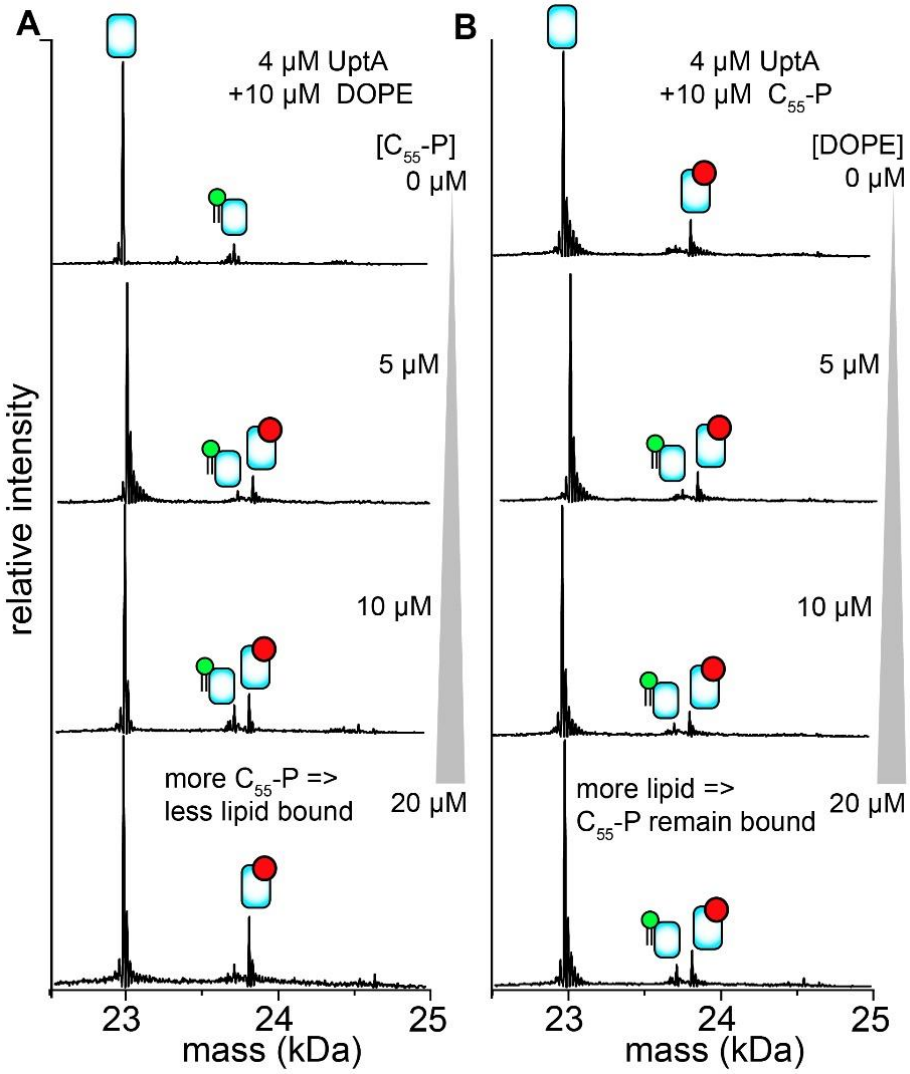

175 **Fig. S7. Competition for UptA between DOPE and C_{55}-P. A.** Deconvoluted mass spectra for
176 solutions containing 4 μM UptA and 10 μM DOPE but different concentrations of C_{55}-P. The DOPE
177 bound to UptA was displaced by the added C_{55}-P. **B.** Spectra for solutions containing 4 μM UptA and
178 10 μM C_{55}-P but different concentrations of DOPE. C_{55}-P remains bound to UptA in the presence of
179 added phospholipids.
180
181
182
183
184
185
186
187

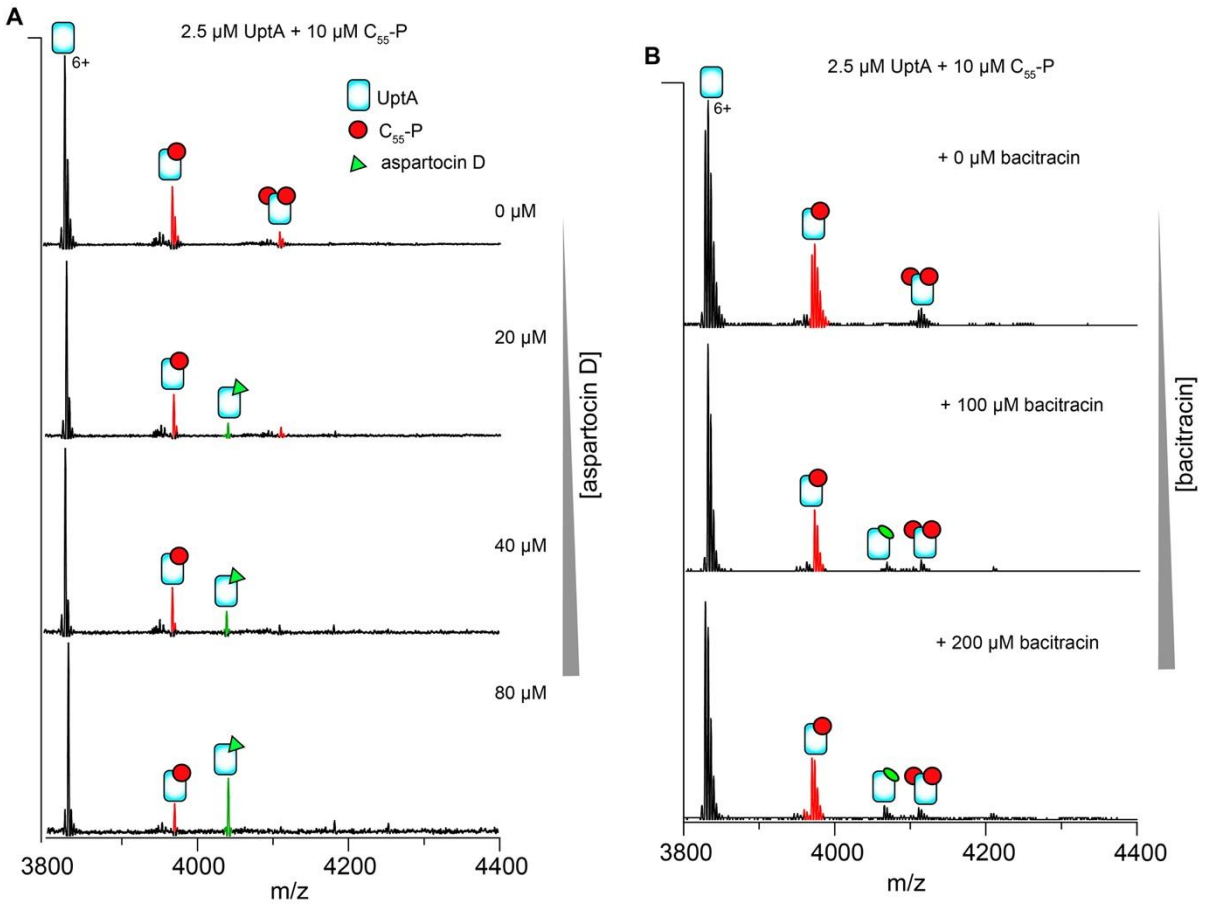

Fig. S8. Aspartocin binds to UptA and disrupts UptA:C_{55}-P interactions. **A.** Spectra (6+ charge state) of 2.5 μM UptA and 10 μM C_{55}-P in the presence of 0-80 μM aspartocin D. Peaks corresponding to UptA: C55-P (highlighted red) decreased in intensity as a function of aspartocin D concentration. **B**. Spectrum recorded for 2.5 μM UptA and 10 μM C_{55}-P but in the presence of 0, 100 and 200 μM bacitracin. Bacitracin binds to UptA only weakly and does not affect C_{55}-P binding.

REFERENCES

1. B. C. Chung *et al.*, Crystal structure of MraY, an essential membrane enzyme for bacterial cell wall synthesis. *Science* **341**, 1012-1016 (2013).
2. A. O. Oluwole *et al.*, Peptidoglycan biosynthesis is driven by lipid transfer along enzyme-substrate affinity gradients. *Nature Communications* **13**, 2278 (2022).
3. M. T. Marty *et al.*, Bayesian Deconvolution of Mass and Ion Mobility Spectra: From Binary Interactions to Polydisperse Ensembles. *Analytical Chemistry* **87**, 4370-4376 (2015).